REPORT DOCUMENTATION PAGE

Form Approved
OMB No. 0704-0188

1. REPORT DATE *(DD-MM-YYYY)*	2. REPORT TYPE	3. DATES COVERED *(From - To)*
20-10-2007	FINAL	01-03-2003 to 31-07-2006

4. TITLE AND SUBTITLE

HIGH MOBILITY CONJUGATED POLYMERS

5a. CONTRACT NUMBER

5b. GRANT NUMBER
F49620-03-1-0162

5c. PROGRAM ELEMENT NUMBER

6. AUTHOR(S)
Samson A. Jenekhe

5d. PROJECT NUMBER

5e. TASK NUMBER

5f. WORK UNIT NUMBER

7. PERFORMING ORGANIZATION NAME(S) AND ADDRESS(ES)

University of Washington, Department
of Chemical Engineering,
Box 351750, Seattle, WA 98195-1750

8. PERFORMING ORGANIZATION REPORT NUMBER

9. SPONSORING / MONITORING AGENCY NAME(S) AND ADDRESS(ES)

Air Force Office of Scientific Research
801 North Randolph Street
Arlington VA 22203-1977

Dr Charles Lee/NA

10. SPONSOR/MONITOR'S ACRONYM(S)
AFOSR

11. SPONSOR/MONITOR'S REPORT NUMBER(S)

12. DISTRIBUTION / AVAILABILITY STATEMENT

Approved for public release; distribution unlimited.

AFRL-SR-AR-TR-08-0031

13. SUPPLEMENTARY NOTES

14. ABSTRACT The performance of all current polymer electronic devices, such as organic field-effect transistors (OFETs), photovoltaic cells, and photodetectors, is limited primarily by the low charge carrier mobilities of current materials. To address this problem this project investigated various polymer semiconductors exhibiting high carrier mobilities and explored their device applications in electronics, optoelectronics, and nanoelectronics. Field-effect electron mobilities as high as 0.1 cm^2/Vs in a spin coated thin films of ladder poly(benzobisimidazobenzophenanthroline) (BBL) were observed. This electron mobility is the highest observed to date in a conjugated polymer semiconductor and was found to vary strongly with intrinsic viscosity (or molecular weight) of the polymer while very stable in air and oxygen. We successfully fabricated and demonstrated a complementary all-polymer inverter for the first time, using p-type poly(3-hexylthiophene) and BBL. A new class of ladder-type bisindoloquinoline semiconductors showing a mobility of 1.0 cm^2 /V.s was synthesized. Ambipolar OFETs were achieved from various p- and n-polymer blends. The field-effect mobility of holes in regioregular poly(3-alkylthiophene)s was found to exhibit a non-monotonic dependence on alkyl chain length, showing a maximum mobility with hexyl. Fundamental insights into the structural factors that govern high mobility charge transport and recombination in polymer semiconductors were also achieved.

15. SUBJECT TERMS
Polymer semiconductor, organic semiconductor, field-effect transistor, ladder polymer, BBL, polymer nanowire, electron transport, light-emitting diode, self-assembly, ladder oligomer, high mobility, eletrospining, polymer blend, ambipolar.

16. SECURITY CLASSIFICATION OF:			17. LIMITATION OF ABSTRACT	18. NUMBER OF PAGES	19a. NAME OF RESPONSIBLE PERSON
a. REPORT	b. ABSTRACT	c. THIS PAGE			19b. TELEPHONE NUMBER *(include area code)*
UNCLASSIFIED	UNCLASSIFIED	UNCLASSIFIED	UNLIMITED	21	

High Mobility Conjugated Polymers

AFOSR Grant no. F49620-03-1-0162

Principal Investigator: Samson A. Jenekhe

Final Report for the Period 01 March 2003 to 31 July 2006

Submitted to the
Air Force Office of Scientific Research
801 North Randolph Street
Arlington VA 22203-1977

By

Professor Samson A. Jenekhe
University of Washington
Department of Chemical Engineering
Benson Hall, Room 105
Seattle, WA 98195-1750
Phone: (206) 543-5525
Fax: (206) 685-3451
E-mail: jenekhe@u.washington.edu

TABLE OF CONTENTS

1. Objectives of Research Project

A fundamental challenge common to all of the current polymer semiconductor devices is to achieve sufficiently high charge carrier mobilities in order to improve the performance of the devices and move them towards practical systems applications. The primary goal of the three-year research project was to address this central problem by exploring current and new ladder polymer semiconductors having high charge carrier mobilities (> 0.01 cm^2/Vs). Although the proposed high mobility polymers are of broad importance to all polymer semiconductor devices, including light-emitting diodes (LEDs), photovoltaic cells, photodetectors, and electrophotographic imaging, we largely focused on their use in thin film transistors (TFTs), organic light-emitting diodes (OLEDs) and related light-emitting transistors (LETs).

The overall goal of the proposed research was to develop next generation high carrier mobility polymer semiconductors and explore their device applications in electronics, optoelectronics, and nanoelectronics. The main objectives of the research are to: (i) develop new conjugated polymer semiconductors having high field-effect mobility of electrons; (ii) establish the relationships between charge carrier mobility and molecular structure and solid state morphology of polymer semiconductors; (iii) develop high-performance n-channel polymer field-effect transistors as suitable switching devices and building blocks for all-polymer integrated circuits for logic, memory, and other functions; and (iv) explore polymer semiconductors that combine efficient light emission with good charge carrier mobilities as precursors to light-emitting transistors (LETs) and ultimately electrically-pumped diode lasers.

To achieve these objectives we developed an integrated research program that encompasses the synthesis of new polymer and oligomer semiconductors, novel processing for realizing nanocrystalline, microcrystalline, and single-crystalline polymer semiconductor thin films, measurement of charge carrier mobilities, and the design, fabrication, and evaluation of high-performance field-effect transistors, OLEDs and light emitting transistors. Our detailed approaches and major research accomplishments are summarized in the following sections. The details are described in the 36 peer-reviewed journal publications arising from this research project to date.

2. Results and Accomplishments

2.1 Ladder Polymer Semiconductors

2.1a High Electron Mobility in Ladder Polymer Field-Effect Transistors. We have observed field-effect electron mobilities as high as 0.1 cm^2/Vs in a solution spin coated conjugated ladder polymer, poly(benzobisimidazobenzophenanthroline) (BBL). These electron mobilities are the highest observed to date in a conjugated polymer semiconductor. Furthermore, the field effect mobility of electrons is several orders of magnitude enhanced in BBL with a ladder architecture compared to its non-ladder conjugated polymer derivative BBB. These results demonstrate that electron transport can be as facile as hole transport in polymer semiconductors, one of the important goals of this research project. These results also represent a major advance towards the development of high performance all-polymer electronics. Indeed, later on in this report we will present results demonstrating the use of BBL as an n-channel organic field-effect transistor (OFET) and a p-type polymer OFET to fabricate and realize the first all-polymer p-n complementary inverters, which are CMOS-like circuit building blocks.

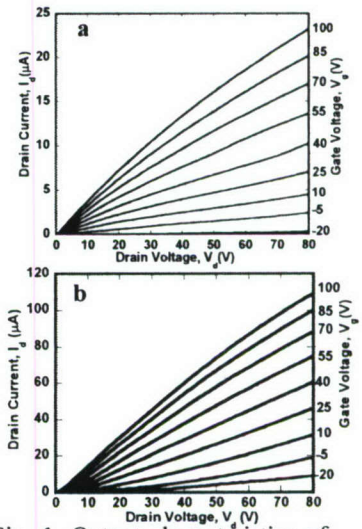

Fig. 1. Output characteristics of BBL FETs with $\mu_{e,sat}$ = 0.03 cm^2/Vs (a) and $\mu_{e,lin}$ =0.1 cm^2/Vs at V_d = 10V(b).

The BBL devices did not show any p-channel characteristics. Instead, typical n-channel FET output characteristics were observed as exemplified in Figure 1. We calculated the field-effect mobility of electrons (μ_e) by using the saturation region transistor equation, $I_d = (W/2L)\mu_e C_o(V_g - V_t)^2$, where I_d is the source-drain current, V_g is the gate voltage, C_o is the capacitance per unit area of the dielectric (SiO_2, 11 nF/cm^2 for the 300-nm thickness)

layer, and V_t is the threshold voltage. BBL FETs annealed at 100 °C for 5 minutes gave a maximum $\mu_{e,sat}$ value of 0.05 cm^2/Vs. A longer annealing period of the same device at 100 °C resulted in an electron mobility of 0.03 cm^2/Vs and an on/off current ratio of 2×10^3. The highest electron mobility in BBL FETs, 0.1 cm^2/Vs calculated using linear region at V_d = 10V, was observed for a device (channel width W = 500 μm, channel length L = 25 μm) in which a siloxane compound, 1,1,1,3,3,3-hexamethyldisilazane, was vapor deposited on top of SiO_2 to promote better adhesion of the spin coated BBL thin film (Figure 1b).

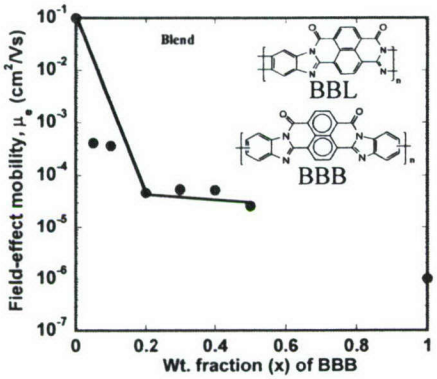

Fig. 2. Composition dependent field-effect mobility of electrons in BBB/BBL blend FETs.

Comparative studies of n-channel FETs made from the structurally related non-ladder BBB and using similar solution processing of thin films gave a maximum electron mobility of 10^{-6} cm^2/Vs. A series of binary blends of BBB and BBL similarly resulted in low field-effect mobilities of order 10^{-5} cm^2/Vs (Figure 2). This finding of several orders of magnitude higher electron mobility in the ladder architecture compared to the otherwise similar but non-ladder conjugated polymer may seem surprising. It is generally assumed that a conjugated ladder polymer would have better π-electron delocalization, and thus also better electronic properties including charge carrier mobility. However, the reason for the observed large difference in electron mobility may not be just because of better π-electron delocalization in the ladder structure as previously thought. Both BBL and BBB have identical optical bandgap (E_g = 1.8 eV) and absorption spectra, electron affinity (EA = ca. 4.0-4.4 eV) and redox properties, and dc conductivity when chemically doped. We find the major difference between the two polymers is morphology; BBL films, spin coated or cast from MSA solutions, were revealed by X-ray and electron diffraction to be semicrystalline whereas BBB films were completely amorphous. AFM images of BBL thin films revealed nanoscale sheets that are randomly oriented within the film. The observed large enhancement of carrier mobility by the ladder architecture of BBL is thus due to the more efficient π-stacking and greater intermolecular order, leading to more crystalline ladder polymer thin films.

2.1b Molecular Weight Dependence of Electron Mobility and Stability of BBL OFETs in Air and Oxygen Atmosphere. We have found that the mobility of electrons in BBL OFETs varies strongly with intrinsic viscosity (or molecular weight) of the ladder polymer (Figure 3). This result confirms a similar finding of dependence of hole mobility on the molecular weight of regioregular poly(3-hexylthiophene). In the case of electron transport in BBL, the increase of electron mobility with increasing molecular weight appears to arise from improved crystallinity and electron delocalization in the ladder polymer. An important implication of this result is that electron mobilities higher than 0.1 cm^2/Vs may be realized if soluble higher molecular weight materials can be synthesized.

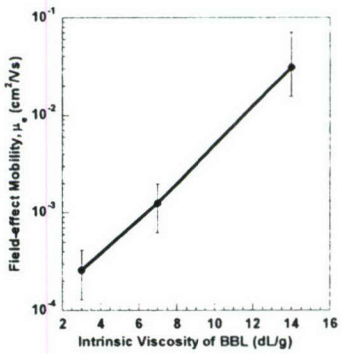

Fig. 3. Effect of molecular weight on FET electron mobility in BBL.

The major challenge in the field of n-type OFETs is to achieve devices that are stable in the presence of ambient air containing oxygen and moisture. Most n-type organic semiconductors are prone to oxidation in the presence of atmospheric oxidants, thus O_2 and H_2O act as efficient electron traps and degrade n-channel OFETs made from current n-type semiconductors. Our systematic study of the effect

of oxygen on the performance of BBL-based field-effect transistors has found the devices to be very stable in air and even oxygen atmosphere.

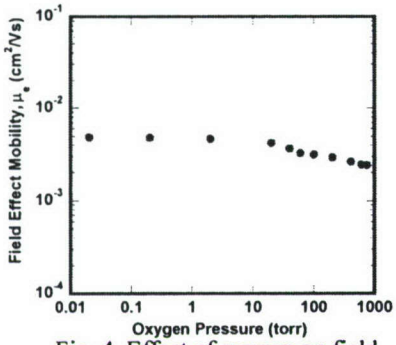

Fig. 4. Effect of oxygen on field effect electron mobility in BBL.

Figure 4 shows a plot of electron mobility in BBL as a function of oxygen pressure (0.2-750 torr). The electron mobility in BBL remained constant from vacuum up to 40 torr of oxygen pressure (0.004 cm^2/Vs) and decreased slightly to 0.0025 cm^2/Vs at 750 torr of oxygen pressure. The excellent stability of the performance of BBL OFETs in oxygen atmosphere is explained by its more positive reduction potential ($E_{red,BBL}$= -0.4 V vs SCE) compared to oxygen ($E_{red,O2}$= -0.9 V vs SCE). In addition to this thermodynamic stability, the strong intermolecular interactions in BBL also provide a kinetic barrier for oxygen transport and interaction with the material.

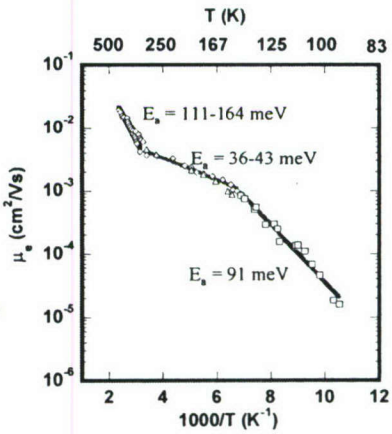

Fig. 5. Temperature dependence of FET electron mobility in BBL.

The temperature dependence of the field-effect mobility of electrons in BBL was also studied over a wide range of temperature (95-423 K). The electron mobility was found to increase from 0.004 cm^2/Vs at room temperature to 0.02 cm^2/Vs at 423 K and decreased to 1.6×10^{-5} cm^2/Vs at 95 K. The increase in field-effect mobility of electrons with increasing temperature shows that the charge transport in BBL is thermally activated. Figure 5 shows the Arrhenius plot of electron mobility versus inverse absolute temperature and the lines represent fits to the data from 95 to 423K. The entire temperature range can be divided into three regions of different activation energies as shown in Figure 5. The ~40 meV activation energy found in the middle temperature region is comparable to that found for hole mobility in regioregular poly(3-hexylthiophene) in the same temperature range.

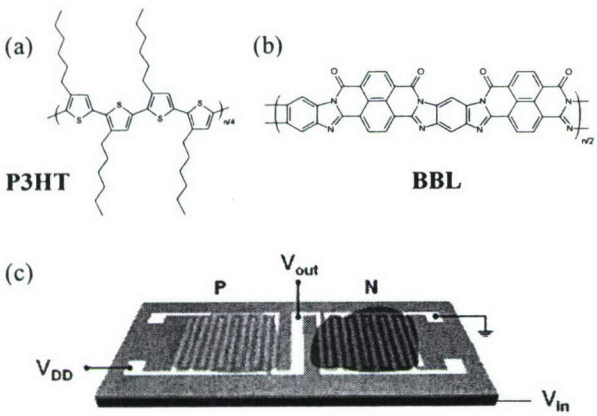

Fig. 6. Chemical structures of (a) P3HT, (b) BBL, and (c) a schematic diagram of the inverter.

2.1c All-Polymer Complementary Inverters. Now that p-channel and n-channel organic field-effect transistors (OFETs) have become available, the next critical step towards low-cost plastic electronics is the integration of p- and n-channel OFETs to achieve functional electronic circuits. Although inverters, based on organic semiconductors have previously been demonstrated, the highly desirable complementary metal-oxide-semiconductor (CMOS)-like polymer inverter for low power dissipation and high performance circuits is yet to be realized. Current graduate students Felix Kim and Alex Briseno have fabricated and demonstrated a complementary polymer inverter for the first time, using p-type poly(3-hexylthiophene) [P3HT, Fig. 6 (a)] and n-type poly(benzobisimidazobenzophenanthroline) [BBL,

Fig. 6 (b)]. A schematic of the all-polymer inverter is shown Fig. 6 (c). Gold source and drain electrodes were patterned on a heavily doped silicon substrate with thermally grown oxide. One side of the substrate was spin coated to produce a BBL thin film. After drying the BBL thin film,

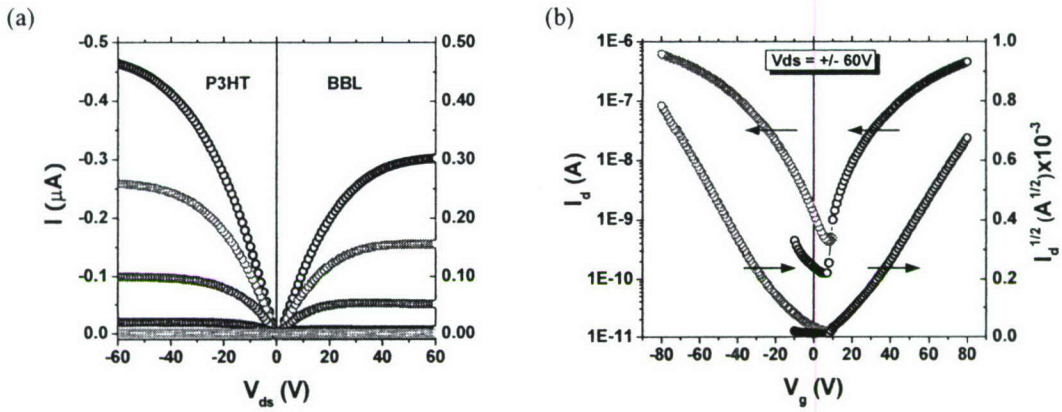

Fig. 7. (a) Output, and (b) transfer characteristics of individual thin film transistors.

the substrate was then spin coated with a P3HT solution and dried (60 °C, in vacuum). Device fabrication and measurement were done in ambient air at room temperature, except during the drying process.

The individual transistors showed typical output and transfer curves expected for p- and n-channel OFETs (see Fig. 7). Carrier mobility for each transistor was about 10^{-4} cm^2 / V s. The p-n complementary inverter showed good noise margins and high voltage gains (Fig. 8). Although the threshold voltage of the inverter was almost half of the supplied voltage, which means it was close to an ideal inverter, there was a small hysteresis caused by the hysteresis of the individual transistors. The maximum gain was larger than 10 when the supplied voltage was 100 V. These results demonstrate the realization of the first all-polymer semiconductor complementary inverters. As expected, the n-channel BBL OFET maintained its mobility and on-to-off current ratio for more than 8 months while the P3HT OFET degraded by several orders of magnitude over the same time. A manuscript reporting these results is being prepared for publication.

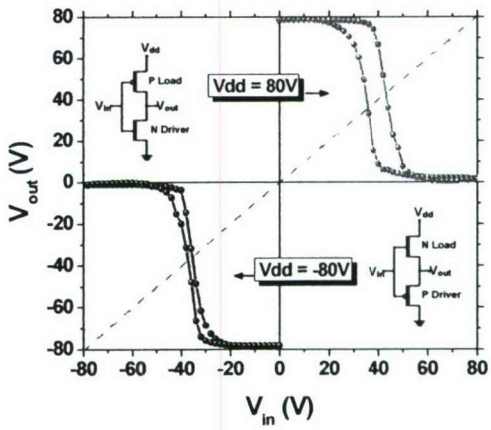

Fig. 8. Voltage transfer characteristics of the complementary inverter.

2.1d BBL Nanowires: Self-Assembly and Nanowire OFETs. Highly oriented BBL nanowires (NWs) were prepared from methanesulfonic acid solutions (0.2 mg/mL) by adding drop wise to a rapidly stirring solution mixture of chloroform and methanol (4:1). The chloroform serves as a weakly interacting solvent while methanol (pka~15) acts as a base to deprotonate the BBL polymer chains, thus enabling the solution-phase self-assembly of BBL nanowires.

It is important to note that if a higher concentration of methanol is employed, then the BBL polymer self-assembles into larger wires. Moreover, if an even larger concentration of methanol is employed, then the concentration of the injecting acidic polymer must be decreased in order to attain nanowires. However, if the acidic polymer solution is added to pure methanol, then there is no formation of nanowires and instead a standard precipitation of BBL structures with no defined morphologies. From Figure 9, the BBL nanowires have a "ribbon-like" one-dimensional morphology as determined from TEM measurements and AFM measurements (not shown). The nanowires have lengths ranging from 20 μm to well over 150 μm. The widths of the nanowires ranged from ~100 nm to ~1 μm, while nanowire thicknesses (determined via AFM measurements) were ~10-50 nm. Such dimensions can be controlled by varying the concentration of the solutions and the quantity of methanol used to precipitate out the nanowires.

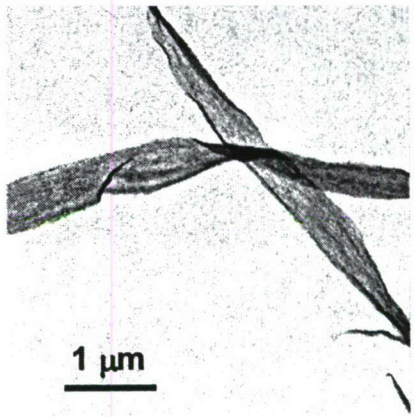

Fig. 9. TEM image of BBL NWs. The widths of the BBL nanowires were ~100 nm to ~1μm and their lengths were ~20-150 μm.

Figure 10A shows a single BBL nanowire bridging the source and drain electrodes of a field-effect transistor. The resulting single-nanowire n-channel transistor showed electron mobilities on the order of 10^{-3} cm^2/Vs and on/off current ratios ~10^4. The output curve (Fig. 10B) exhibits well-resolved saturation currents with excellent modulation as the gate voltage is increased from

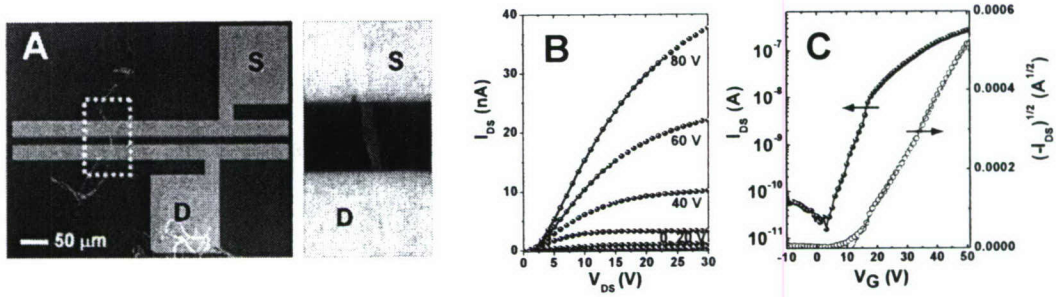

Fig. 10. (A) A single BBL nanowire OFET and a close-up showing the nanowire bridging the source-drain electrodes. (B) Output characteristics showing well-resolved current-voltage saturation. (C) The corresponding transfer and square root of current characteristics. The single NW OFET has a ~0.001 cm^2/Vs mobility and on/off current ratio of ~10000. All measurements on NW transistors were performed under ambient air.

0 to 80 V. Figure 10C shows a plot of the log and square root of drain current as a function of gate voltage (V_G). The transfer curve shows an increase in current by more than 4 orders of magnitude as the voltage is ramped from -10 to 50 V. The square-root of drain current follows the square law and the fitting line used for calculating mobility fits the data over a wide range of gate voltage values. These results are comparable to those reported from p-channel single poly(3-hexylthiophene) nanowire OFETs (Merlo, J. A. et al. *J. Phys. Chem. B.* **2004**, *108*, 19169). Therefore, our current results may open the possibility of fabricating all-polymer nanowire integrated circuits. A manuscript describing these BBL NWs and nanowire OFETs has been prepared and will be submitted to JACS.

2.2 High Mobility New Ladder Bisindoloquinoline Semiconductors

We have designed and synthesized a new class of ladder-type conjugated oligomers, bisindoloquinolines, exemplified by the tetra-phenyl derivative TPBIQ shown below (Fig. 11). Graduate student Eilaf Ahmed used a novel synthetic route involving intramolecular cyclicization to make TPBIQ and derivatives. Single crystal X-ray diffraction revealed a crystal structure with excellent π-π stacking, which can facilitate efficient charge transport. As a p-channel semiconductor in field-effect transistors, the TPBIQ semiconductor had a mobility of 1.0 cm^2 /V.s with on/off current ratios exceeding 10^4 (see Fig. 11). These results are particularly important for several reasons. (1) In contrast to extensively studied pentacene and related polyacenes, bisindoloquinolines represent an entirely new class of polycyclic oligomers, incorporating heteroatoms, that show high carrier mobility. (2) The observed π-stacking in TPBIQ also contrasts with the herringbone crystal structure of pentacene. (3) The synthetic chemistry is a simple and flexible high-yielding route that can generate many derivatives, and thus should facilitate structure-carrier mobility correlations. (4) As observed with rubrene and other organic semiconductors, further purification and crystallization could lead to much higher carrier mobilities (> 1 cm^2 /V.s). A manuscript reporting these results has been submitted to JACS.

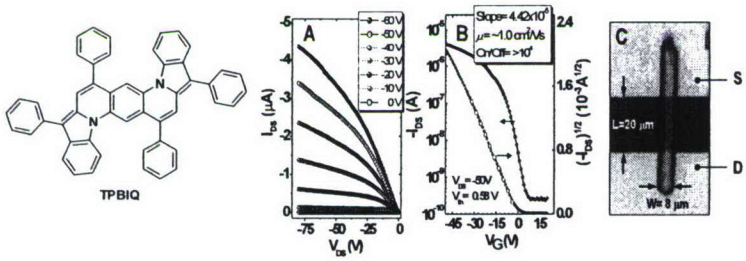

Fig. 11. Molecular structure of **TPBIQ** and (A) output and (B) transfer characteristics of **TPBIQ** single crystal transistor. (C) Optical micrograph of the single-crystal OFET. The W/L of the OFET active are is ~0.4.

2.3 Self-Assembled Polymer Nanowires with High Ambipolar Carrier Mobilities

Among synthetic polymers it is very rare for two chemically different polymers to self-assemble or cocrystallize when mixed; rather, they generally phase separate. We have discovered that binary blends of regioregular poly(3-hexylthiophene) (P3HT) and our recently synthesized regioregular poly(4-hexylquinoline) (P4HQ) in dilute chloroform solutions self-assemble into crystalline nanowires with a mean diameter of 19 nm and lengths of order 5-10 μm. The molecular structures of P3HT and P4HQ are shown in Figure 12 and representative transmission electron microscope (TEM) images of the nanowires are shown in Figure 13.

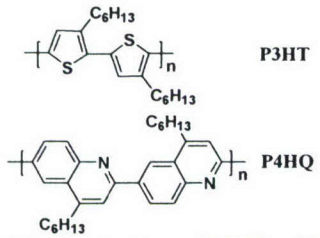

Fig. 12. Molecular structures of P3HT and P4HQ.

X-ray diffraction patterns of films of blend nanowires and both homopolymers cast from chloroform are shown in Figure 14A. The X-ray diffraction patterns of the blend nanowires give strong first-order reflections at 2θ angle of 5.39-5.42° indicating that the two polymers cocrystallize into highly ordered layered structures with an interlayer d-spacing of 16.30-16.40 Å (Figure 14B). Additionally, second-order and third-order reflections were observed in the blend nanowires and P3HT homopolymer due to the highly ordered structures. The weak and broad peaks in the diffraction patterns centered at around 23° are assigned to the interchain π-stacking distance corresponding to a spacing of about 3.87 Å.

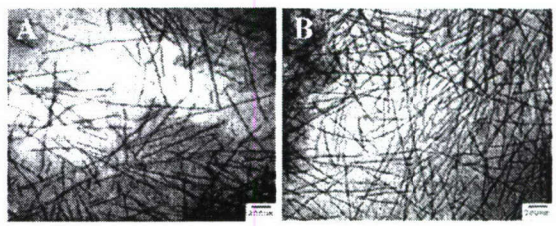

Fig. 13. TEM images of self-assembled P3HT/P4HQ blend nanowires on copper grids. (A) 5, and (B) 20 wt % P4HQ in binary blends self-assembled in 0.5 wt % chloroform solutions.

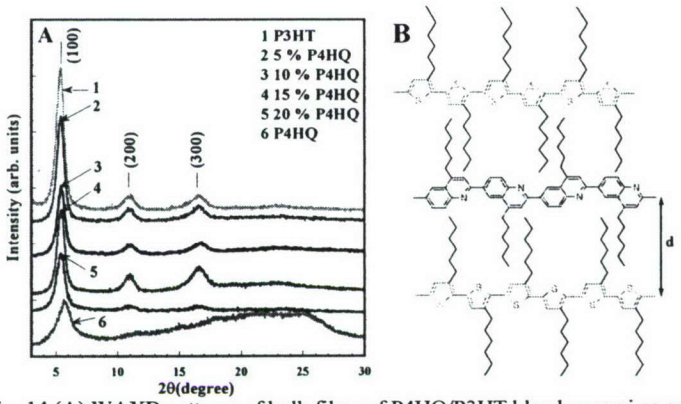

Fig. 14 (A) WAXD patterns of bulk films of P4HQ/P3HT blend nanowires and both homopolymers and (B) Schematic of layered structures of blend nanowires.

We investigated the charge transport properties of bulk thin films of the polymer nanowires in field-effect transistors and observed ambipolar charge transport of holes and electrons (Figure 15). From the p- and n-channel field-effect transistor (FET) output characteristics for the 20 weight % P4HQ blend nanowires (Fig. 15A,B), we obtained hole and electron mobilities of 0.012 cm^2/Vs and 0.004 cm^2/Vs, respectively, in the linear region. The hole mobility in these bulk films of the blend nanowires is very close to that of cast films of the pure P3HT (0.02-0.05 cm^2/Vs). If the fact that the web of nanowires occupy only 6% of the FET channel area is taken into account, the calculated carrier mobilities become 0.2 cm^2/Vs for holes and 0.067 cm^2/Vs for electrons. Observation of electron transport in the nanowires confirms the presence of the electron-transporting P4HQ in the blends. The high ambipolar carrier mobilities in the blend nanowires imply cocrystallization of the components. Since field-effect mobility of electrons is otherwise not measurable in pure P3HT, the observation of electron and hole transport in these nanowires demonstrates that blending is an important approach to modifying the electronic properties of conjugated polymer semiconductors analogous to doping in inorganic semiconductors.

The novel self-assembly approach to polymer nanowires with nano-scale cross-sections and lengths on the order of micrometers from binary blends of conjugated polymers may be applicable to other polymer blend systems. It opens up opportunity for exploring the applications of blends of conjugated polymers in future nanoscale and molecular electronic devices. It also represents a very rare example of a pair of chemically different polymers that self-assemble and cocrystallize. As such it should be of broad interest in polymer science and supramolecular chemistry.

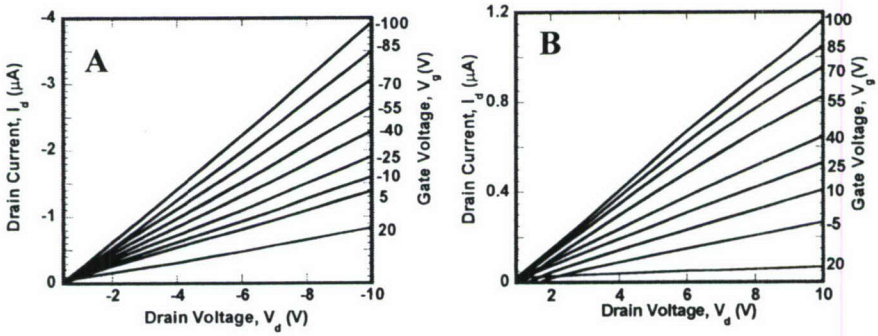

Fig. 15. Output characteristics of a P3HT/20 wt% P4HQ nanowire FET: (A) p-channel and (B) n-channel mode.

2.4 Field-Effect Charge Transport in Blends of Polymer Semiconductors

2.4a Ambipolar OFETs fron BBL/CuPc Blends. Ambipolar polymer FETs, which can operate in both p- and n-channel modes, are of great interest for developing low-power complementary integrated circuits for logic and memory applications. Ambipolar charge transport is also important for developing electrically pumped light emitting devices. However, current organic and polymer semiconductors do not show ambipolar charge transport properties. We have explored polymer blend approach in which a p-type component and an n-type component are combined to create ambipolar polymer blends. A promising blend system we have investigated consists of n-type BBL and the p-type small molecule, copper phthalocyanine (CuPc), whose structures are shown in Figure 16.

The morphology of BBL-CuPc blend thin films was investigated using transmission electron microscopy (TEM) in both image mode and selective area diffraction mode. The bright field TEM images of BBL-CuPc blend thin films (Figure 17) showed composition-dependent nanophase-separated morphologies. Figure 17a shows the TEM micrograph of a 35 wt% CuPc blend thin film processed from water, to extract methanesulfonic acid (MSA), the common solvent used to make the blend solutions, whereas Figure 17b is of those processed from methanol. In blend thin films processed from water, CuPc

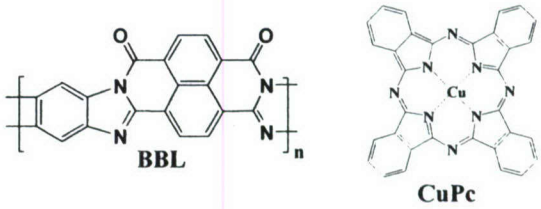

Fig. 16. Molecular structures of binary blend components (BBL and CuPc).

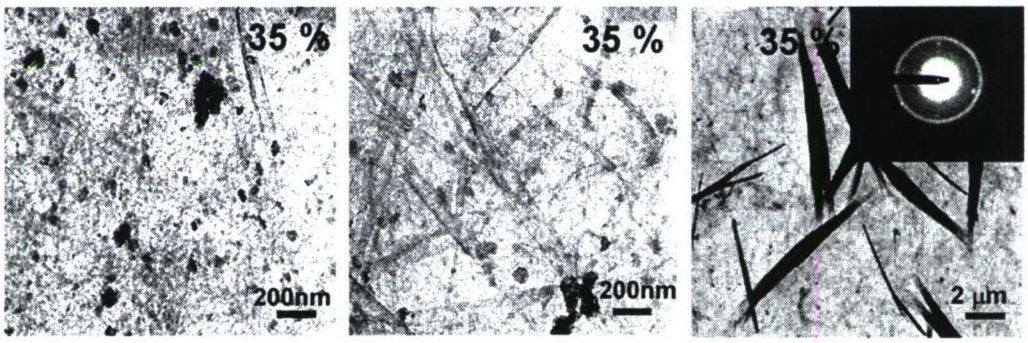

Fig. 17. TEM micrographs of a 35 wt% CuPc blend. Films processed from water (a), methanol (b) and vapor annealing in methylene chloride for 55 h (c).

forms aggregates of non-uniform size distribution, which ranges from 50-200 nm. These aggregates are believed to be the α-crystalline form of CuPc. Electron diffraction of these water-extracted films showed the polycrystalline diffraction rings corresponding to BBL, but diffraction spots/rings corresponding to CuPc were not seen. However, when the MSA was extracted in methanol, the films showed formation of elongated, plate-like domains of CuPc (Figure 17b) along with the globular-like aggregates. The length of these elongated platelets ranges from 1µm to 5 µm, whereas the width ranges from 50 nm to 100 nm. The number density of these elongated platelets increased with an increase in CuPc concentration. More evident phase separated morphology is seen when these films, after MSA extraction in methanol, were subjected to solvent-vapor annealing in methylene chloride vapor. After 6 h of annealing in methylene chloride vapor, CuPc self-assembled into 1-3 µm long, needle-like domains corresponding to the β-form of CuPc, with some remaining globular aggregates. These elongated self-assembled domains of CuPc grow in all three dimensions with longer annealing times and the number density of globular-like aggregates decreased. Figure 17c shows TEM micrographs of 35 wt% CuPc blend films as a representative morphology of BBL-CuPc blends after 55 h of annealing in methylene chloride vapor. The vapor annealed blend films have well developed self-assembled domains of CuPc with sharp grain boundaries whereas the methanol extracted blends films showed under developed and diffuse grain boundaries. Selective area electron diffraction patterns of methylene chloride vapor annealed blend films are shown in the inset of Figure 17c. The spots that appear after annealing correspond to single crystals of β-form CuPc superimposed on the polycrystalline diffraction rings of BBL.

Typical output characteristics of BBL-CuPc FETs operating in both the hole-enhancement mode and electron-enhancement mode are shown in Figure 18 for ambipolar devices processed from methanol. Figure 18a shows the output characteristic of a 35 wt% CuPc blend transistor operating in n-channel mode. For high gate voltages, the transistor operates in the n-channel mode with a field-effect mobility of 7×10^{-5} cm^2/Vs calculated from the saturation regime (V_d = 50 V). For low gate voltages and high drain

voltages, the I_d showed a non-linear increase, typical of ambipolar transistors, due to the formation of p-n junction in the channel region. At negative gate voltages, the same FET operates in p-channel mode (Figure 18b) with a hole mobility of 8×10^{-5} cm^2/Vs measured in the saturation region.

These results demonstrate that ambipolar thin film transistors that are stable in air can be developed from solution-processed polymer blends. Although the present ambipolar carrier mobilities are low compared to unipolar FET mobilities, we believe that optimization of blend composition, processing, and morphology will allow significant improvement.

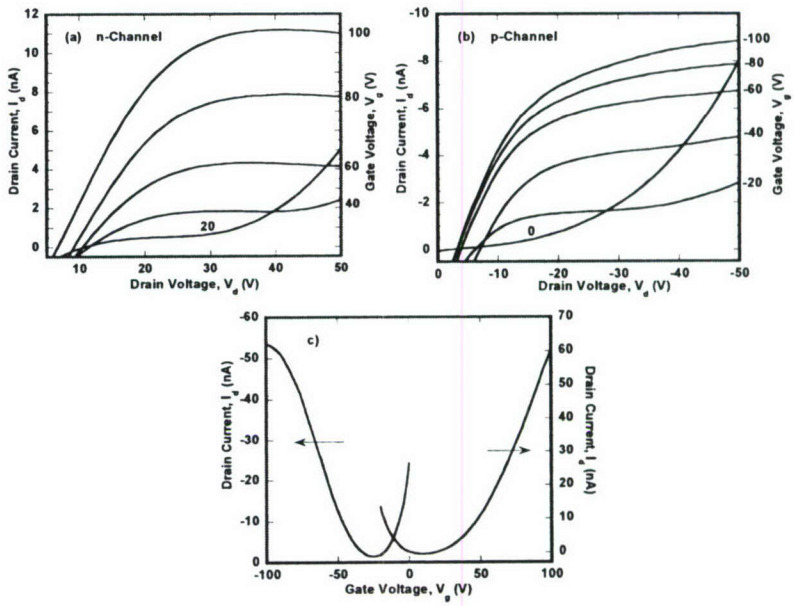

Fig. 18. The output (a,b) and transfer (c) characteristics of a 35 wt% CuPc blend FET showing ambipolar operation in electron enhancement mode (a) and hole enhancement mode (b).

2.4b n-Channel and Ambipolar OFETs from BBL/PTHQx Blends. In the growing field of organic electronics, including OFETs and solar cells, the need to develop materials which can support both holes and electrons is of great interest. To continue our quest for new ambipolar polymer semiconductors and to understand the interplay between morphology and charge transport, we have studied a series of 10 binary blends of n-type BBL and p-type thiophene-quinoxaline copolymer (PTHQx) ranging between 10-80 wt% PTHQx.

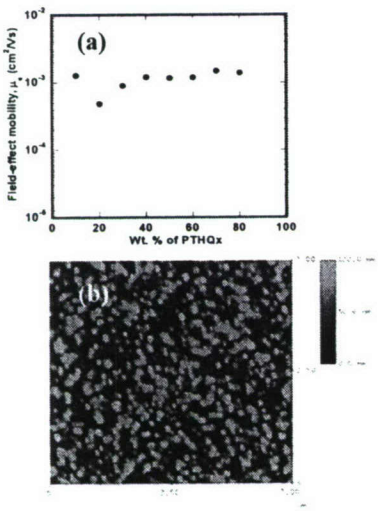

Fig. 19. Compositional dependence of the electron mobility in BBL/PTHQx blends (a) and AFM topographic image of a 50 wt % blend thin film (b).

Surprisingly, all the blend OFETs in the 10-80 % composition range showed n-channel transistor characteristics and no p-channel activity was observed in any of these blend compositions. Figure 19a shows the electron mobility in these blend FETs as a function of blend composition. The field-effect mobility of electrons in the 10-80 wt% composition range is found to be relatively high and constant at about 1×10^{-3} cm^2/Vs. It should be noted that the electronic structures of the two blend are such that neither of the component will act as a trap for opposite charge carriers; the electron affinities were 4.0 eV (BBL) and 2.7 eV (PTHQx) and ionization potentials were 6.0 eV (BBL) and 5.0 eV (PTHQx).

Figure 19b shows a topographic atomic force microscopy (AFM) image of a 50 wt% blend thin film. AFM of all the BBL/PTHQx blend thin-films revealed a phase-separated morphology with phase separation on the length scale of 100–250 nm. Even though the phase-separated morphology is appropriate for observing ambipolar charge transport in the polymer blends, our observation of only electron transport does not currently have an explanation. Ambipolar charge transport was observed in this blend system at a very high concentration

of the p-type semiconductor (≥ 90 wt % PTHQx). Ambipolar charge transport is exemplified by an electron mobility of 1.4×10^{-5} $cm^2/(V\ s)$ and a hole mobility of 1.0×10^{-4} $cm^2/(V\ s)$ observed in the 98-wt % PTHQx blend field-effect transistors. These results show that ambipolar charge transport and the associated carrier mobilities in blends of conjugated polymer semiconductors have a complex dependence on the blend composition and the phase-separated morphology. These results also point to the need to explore donor-acceptor copolymers as a more fundamental approach to ambipolar OFET materials.

2.4c Charge Transport in Electrospun Polymer Blend Nanofibers. We have demonstrated that conjugated polymers such as poly[2-methoxy-5-(2-ethylhexyloxy)-1,4-phenylenevinylene]) (MEH-PPV) and its blends with poly(3-hexylthiophene) (PHT) could be readily fabricated as uniform nanofibers by co-electrospinning their solutions with another solution containing poly(vinyl pyrrolidone) (PVP) (Figure 20) through a coaxial capillary system, followed by extraction of the PVP phase with ethanol. The morphology and diameter of the final nanofibers can be varied by controlling the experimental parameters, such as solution feed rates and solution concentration.

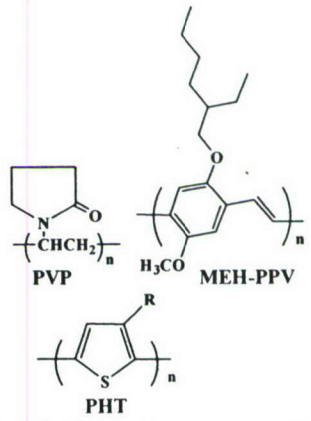

Fig. 20. Molecular structures of polymers.

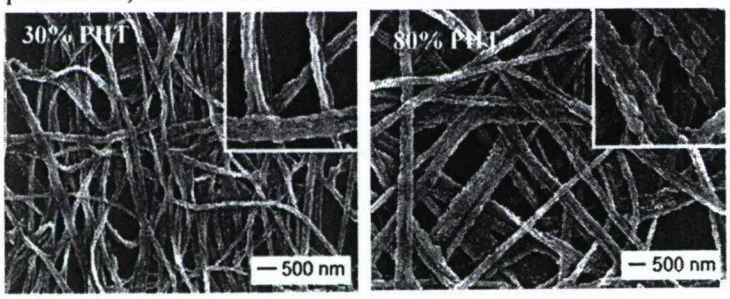

Fig. 21. SEM images of MEH-PPV/PHT blend nanofibers with different contents of PHT.

Figure 21 shows typical SEM images of MEH-PPV/PHT blend fibers with different contents of PHT. The presence of PHT in these nanofibers was also confirmed by energy-dispersive X-ray (EDX) analysis. Compared to pure MEH-PPV fibers, the surfaces of these blend fibers were much rougher. It can be seen that these fibers are mainly composed of small particles with dimensions in the range of 30 to 50 nm.

For both MEH-PPV and MEH-PPV/PHT blends, the optical absorption peak of electrospun nanofibers is slightly red shifted as compared to the thin films. In addition, the absorption band of the nanofibers is broadened, suggesting a more inhomogeneous environment. The red shift in the absorption peak implies that there is a shift in chain distribution within each nanofiber towards more extended polymer chains and better delocalized π-conjugation. The emission spectra taken from MEH-PPV/PHT blend nanofibers showed a more efficient energy transfer process from MEH-PPV to PHT due to the stronger interaction between MEH-PPV and PHT in these confined nanostructures as compared to the bulk thin films (Figure 22).

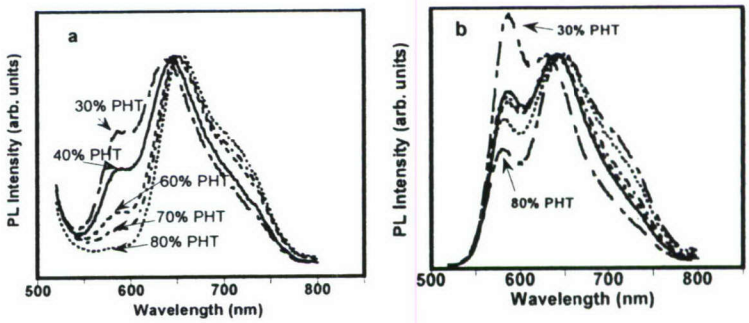

Fig. 22. Photoluminescence spectra taken MEH-PPV/PHT blend nanofibers (a) and spin-cast thin films (b).

We fabricated and investigated field-effect transistors based on MEH-PPV/PHT blend nanofibers. Figure 23a shows an output characteristic of an 80 % PHT blend FET. The I-V curves show a typical *p*-channel operation with field-effect mobility of holes of 1×10^{-4} cm^2/Vs. Compositional dependence of field-effect mobility in these blend nanofibers is shown in Figure 23b. Compared to the hole mobility in 80% PHT nanofibers there is more than an order of magnitude decrease in the hole mobility when 30% PHT (5×10^{-6} cm^2/Vs) is present in the nanofiber blend. This calculation of mobility is done with the physical channel width (W) of the device, which clearly yields the lower bound of carrier mobility since the conduction area between source and drain electrodes is not fully covered by the nanofiber mesh.

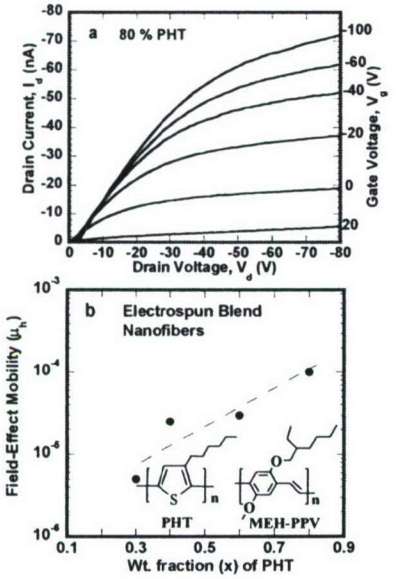

Fig. 23. Output characteristic of a blend nanofiber FET (a) and compositional dependence of field-effect mobility of holes in blend nanofibers (b).

We have demonstrated that nanofibers of conjugated polymers and their blends could be conveniently fabricated by electrospinning. Furthermore, we have fabricated field-effect transistors based on these nanofibers and used them to study charge transport in well-defined 1-D polymer nanostructures.

2.5 Structure-Carrier Mobility Relationships in Polymer Semiconductors

2.5a Alkyl Chain Length Dependence of the Carrier Mobility in Regioregular Poly(3-alkylthiophene)s. The field-effect mobility of holes in regioregular poly(3-alkylthiophene)s was determined for a series of 5 alkyl chain lengths from C_4 (n-butyl) to C_{12} (n-dodecyl) by a systematic investigation of thin film transistors. A non-monotonic dependence of field-effect mobility on alkyl chain length was found, showing a maximum mobility with hexyl (Figure 24). The average hole mobility varied from 1.2×10^{-3} cm^2/Vs in poly(3-butylthiophene) and 1.0×10^{-2} cm^2/Vs in poly(3-hexylthiophene) to 2.4×10^{-5} cm^2/Vs for poly(3-dodecylthiophene). Because the hopping probability of charge carriers is a decreasing exponential function of hopping distance, one can expect the hole mobility to decrease monotonically with alkyl chain length. However, our experimental observation shows that the hole mobility as a function of alkyl chain length has a peak at hexyl side chain, resulting in $\mu_{PHT} > \mu_{PBuT}$. This experimental result suggests that the hole mobility is a function of not only the interlayer distance but also other morphological variables such as the degree of crystallinity, crystallite size, etc. The hexyl side group appears to best optimize these variables for hole transport among the regioregular poly(3-alkylthiophene)s. The present results provide an important structure–carrier mobility relationship for the regioregular poly(3-alkylthiophene)s which are of wide interest for thin film transistors and photovoltaic cells. This alkyl chain length dependence of charge transport will also be important for other regioregular conjugated polymers such as the poly(4-alkylquinoline)s or poly(dialkylfluorene)s.

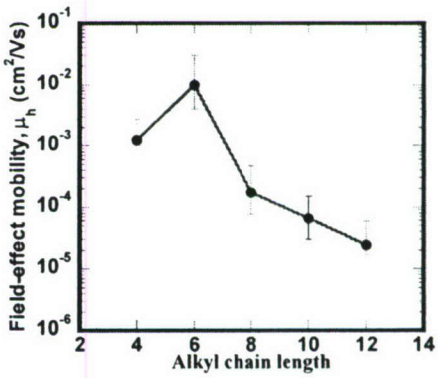

Fig. 24. Dependence of hole mobility on the alkyl chain length of regioregular poly(3-alkylthiophene)s.

2.5b Thiophene- Based Donor-Acceptor Copolymers for Field-Effect Transistors. Our recent results which demonstrated ambipolar field-effect transistors based on blends of donor and acceptor polymers suggested that conjugated polymer semiconductors with donor-acceptor architectures could in principle be expected to exhibit ambipolar charge transport with high carrier mobilities if the electronic structures and solid-state morphologies of the materials are better understood and controlled. If realized, such ambipolar polymer semiconductors could find applications in thin film transistors, CMOS-type electronic circuits, and novel types of organic solar cells not limited by exciton diffusion length.

Thiophene-based donor-acceptor conjugated copolymers are particularly interesting to explore since their electronic and optoelectronic properties could be tuned efficiently by intramolecular charge transfer (ICT). However, although some thiophene-based donor-acceptor conjugated copolymers have previously been synthesized, little is known about their field-effect charge carrier transport properties. We have thus carried out a joint experimental and theoretical investigation of the electronic properties, thin-film morphology and field-effect transistor characteristics of a thiophene-quinoxaline conjugated copolymer, poly[(thiophene-2,5-diyl-*alt*-(2,3-diheptyl quinoxaline-5,8-diyl)] (PTHQx) shown in Figure 25. The theoretical electronic structures and properties of the related poly(thiophene-2,5-diyl-*alt*-thieno[3,4-b]pyrazine)(PTTP) were also investigated by density functional theory (DFT) with the goal of understanding the effect of intramolecular charge transfer on the electronic structure and field-effect charge carrier transport. A hole mobility of 3.6 x 10^{-3} cm^2/V s and an on/off current ratio of 6 x 10^5 were observed in initial p-channel OFETs made from spin-coated PTHQx thin films (Figure 26). Atomic force microscopy of PTHQx thin films showed a novel polycrystalline grain morphology that varied with the substrate surface. This morphology of PTHQx thin films is reminiscent of that commonly observed for thermally evaporated small molecule semiconductors such as pentacene. One implication of the polycrystalline grain morphology of PTHQx thin films is that advances in processing this copolymer could directly improve OFETs made from it as has been observed for pentacene.

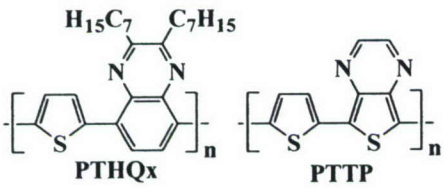

Fig. 25. Molecular structures of the donor-acceptor copolymers.

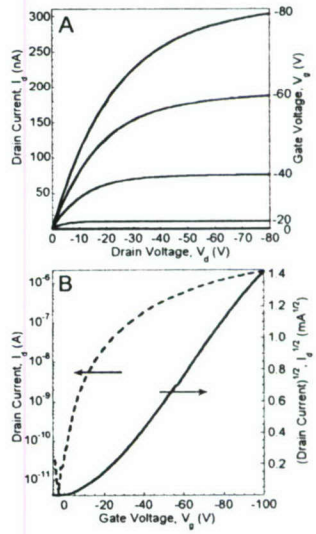

Fig. 26. Output (A) and transfer (B) characteristics of a **PTHQx** OFET.

The electronic structures of PTHQx and PTTP calculated by the density functional theory showed LUMO levels of -2.73 and -3.42 eV, respectively, and small effective masses (0.11-0.23 m_e). PTTP is thus an excellent candidate for synthesis and is predicted to have superior properties. Our combined experimental results and DFT calculations provide a rational methodology for designing new conjugated polymers with donor-acceptor architectures for meeting the requirements for high charge carrier mobilities and ambipolar charge transport for transistors and other organic electronics.

2.5c Phenoxazine-Based Conjugated Polymers and Oligomers for Field-Effect Transistors. One of the key objectives of our synthetic efforts is to develop new building blocks for the design of high mobility semiconductors for organic field-effect transistors (OFETs) and other organic electronic devices. Although the tricyclic phenoxazine ring has not previously be used in the design of organic or polymer semiconductors, it is potentially better compared to the widely used carbazole ring or even phenothiazine which we reported on recently. The ionization potential of phenoxazine is 0.7 eV lower compared to that of carbazole and this means its radical cations (or holes) are more stable. On the other hand it is relatively more planar and

more resistant to irreversible oxidation than phenothiazine. We have thus synthesized several phenoxazine-based π-conjugated polymers, including poly(10-hexylphenoxazine-3,7-diyl-*alt*-3-hexylthiophene-2,5-diyl) (POT) (Figure 27). These polymers have high glass transition temperatures (112-230 °C) and highly reversible electrochemical oxidation and low ionization potentials (4.9 eV).

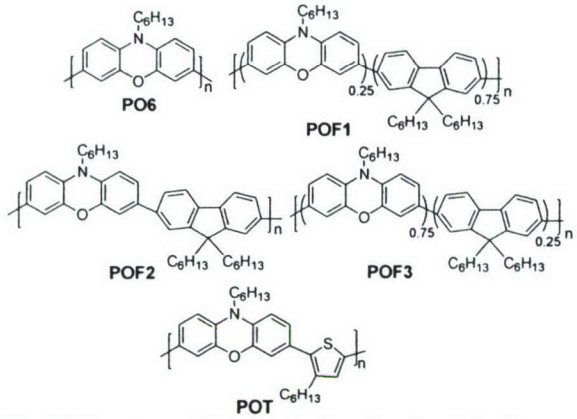

Fig. 27. Structures of phenoxazine-based conjugated polymers.

Thin-film transistors based on polyphenoxazine and its copolymers showed typical p-channel output characteristics with good drain current modulation and well-defined linear and saturation regions when operated in accumulation mode. Figure 28 shows the output and transfer characteristics of thin film transistors based on POT. A maximum hole mobility of 6×10^{-4} cm^2/Vs and on/off ratio of 10^4 was measured. Our results show that the low ionization potential (4.9 eV) of the phenoxazine-containing copolymers facilitates hole injection and transport in OFETs. An article based on these results has been published.

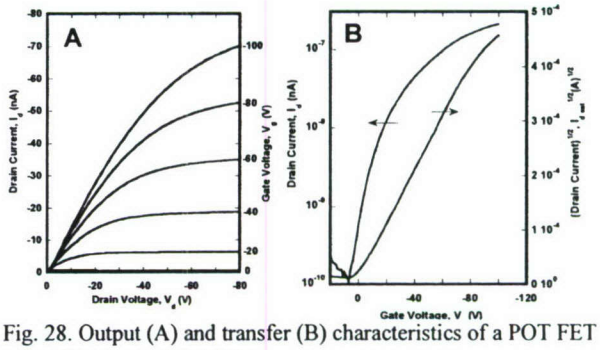

Fig. 28. Output (A) and transfer (B) characteristics of a POT FET with OTS-18-modified SiO_2.

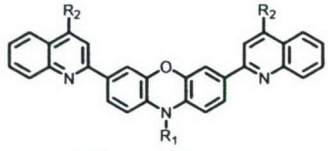

R_1= ◯ , R_2 = ◯ **(BPQ-PPO)**

R_1= CH_3 , R_2 = ◯ **(BPQ-MPO)**

R_1= ◯ , R_2= CH_3 **(BMQ-PPO)**

R_1= CH_3 , R_2= CH_3 **(BMQ-MPO)**

Fig. 29. Structures of phenoxazine-based donor-acceptor molecules.

Four new donor-acceptor (D-A) molecules (Figure 29) incorporating phenoxazine as the donor and quinoline as the acceptor were synthesized, characterized, and explored in organic light-emitting diodes (OLEDs) and OFETs. The phenoxazine-based D-A molecules had high glass transition temperatures of up to 150 °C. Bright and efficient green OLEDs were achieved from the intramolecular charge transfer (ICT) fluorescence of the D-A molecules. The current density-voltage-luminance characteristics of an ITO/PEDOT/TAPC /BPQ-PPO/LiF/Al device are shown in Figure 30A. The diode had a low turn-on voltage (3.0 V), a maximum brightness of 9510 cd/m^2, a maximum external quantum efficiency (EQE) of 10% at 6580 cd/m^2 and a luminous efficiency of 3.42 cd/A.

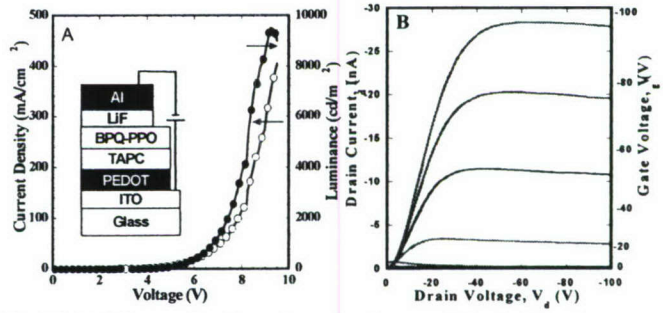

Fig. 30. (A) Current density-voltage-luminance of the devices shown in the inset and (B) output characteristics of a BMQ-PPO FET.

The saturation region field effect mobility of holes in BMQ-PPO was found to be 7×10^{-4} cm^2/Vs whereas it was 8×10^{-5} cm^2/Vs in BPQ-MPO and 3×10^{-5} cm^2/Vs in BPQ-PPO. These OFETs and

OLEDs results demonstrate that efficient light-emitting transistors could be achieved if phenoxazine-based semiconductors are incorporated into appropriate device structures.

2.4d New Oligoquinoline: High Electroluminescence Efficiency and p-Channel Field Effect Charge Transport. Quinoidal oligothiophenes with π-stacked solid state structures were recently found to be good n-channel semiconductors for OFETs, showing electron mobilities as high as 0.2 cm^2/Vs. We are interested in exploring electron-deficient rings, such as 4-phenylquinoline, as building blocks for new quinodimethane compounds that may be capable of ambipolar charge transport and high luminescence efficiency. This is one possible approach to light emitting transitors.

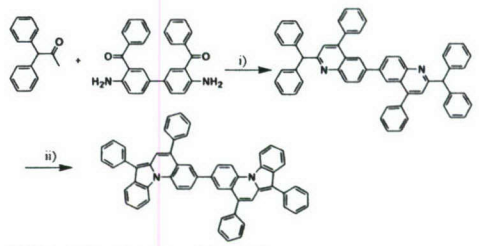

i) Diphenyl phosphate, toluene 120 C, 24 h.
ii) 2,3-Dichloro-5,6-dicyano-1,4-benzoquinone, MeCN, reflux 24 h.

Fig. 31. Synthesis of BQPQ compound.

We designed and attempted to synthesize a novel tetraphenylquinodimethane based on electron-deficient 4-phenylquinoline oligomer. However, instead of the expected quinoidal oligomer we obtained the novel BQPQ compound shown in Figure 31 as confirmed by single crystal X-ray structure. We explored the highly fluorescent BQPQ molecule in organic light emitting diodes and thin film transistors. BQPQ displayed an unusually low ionization potential (5.0 eV) and was thus used as a p-channel semiconductor in thin film transistors and as a emitter to achieve very bright and high efficiency green light-emitting diodes.

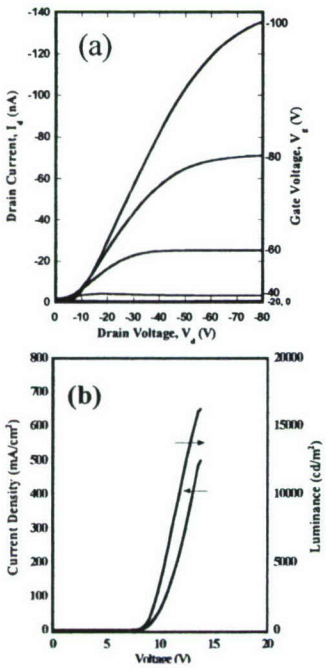

Fig. 32. (a) Output characteristics of a BQPQ FET and (b) current density-luminance-voltage curves of a BQPO diode.

Bottom contact organic field effect transistors (OFETs) fabricated from gold source/drain electrodes, SiO_2 gate dielectric layer, and vacuum evaporated BQPQ thin films showed typical p-channel output characteristics with good drain current modulation and well-defined linear and saturation regions when operated in accumulation mode (Figure 32a). The saturation region mobility of holes was 4×10^{-4} cm^2/Vs with an on/off ratio of 10^3. Very bright and efficient green electroluminescent diodes were realized from BQPQ. The device architecture of ITO/PEDOT/PVK/BQPQ/TPBI/LiF/Al showed the best performance with a brightness of 16255 cd/m^2 (Figure 9b). The maximum external quantum efficiency (EQE) was 1.9 % at a brightness of 2035 cd/m^2 with a luminous efficiency of 5.9 cd/A.

Future work will aim to synthesize tetracyano and other derivatives of BQPQ oligomer as semiconductors for ambipolar thin film transistors, high performance OLEDs, and light emitting transistors. It would be interesting to achieve single-crystal BQPQ OFETs.

2.4e Polyphenothiazine Field-Effect Transistors. The electron-rich ring of phenothiazine makes it an excellent building block for achieving low ionization potential (IP) conjugated polymers. The low-IP phenothiazine-based polymers can thus be good candidates for hole conduction in field-effect transistors. Carbazole-based conjugated polymers have been shown to be good p-type semiconductors. One important difference between the phenothiazine and carbazole rings is the planarity. The carbazole ring is planar whereas the phenothiazine ring is highly non-planar (dihedral angle ~ 158.5°). Non-planarity may lead to poor π-stacking. To understand the effect of molecular planarity, and thus efficient π-stacking, on charge carrier mobility, we have investigated field-effect transistors based on phenothiazine-based conjugated polymers synthesized in our group: poly(10-hexylphenothiazine-3,7-diyl) (PHPT), poly(10-hexylphenothiazine-3,7-diyl-*alt*-3-hexylthiophene) (HPT-HT) and poly(10-hexylphenothiazine-3,7-diyl-

alt-3,4-dihexylthiophene) (HPT-DHT). We have also studied poly(N-hexylcarbazole-3,6-diyl) (PHCz) for comparison (Figure 33).

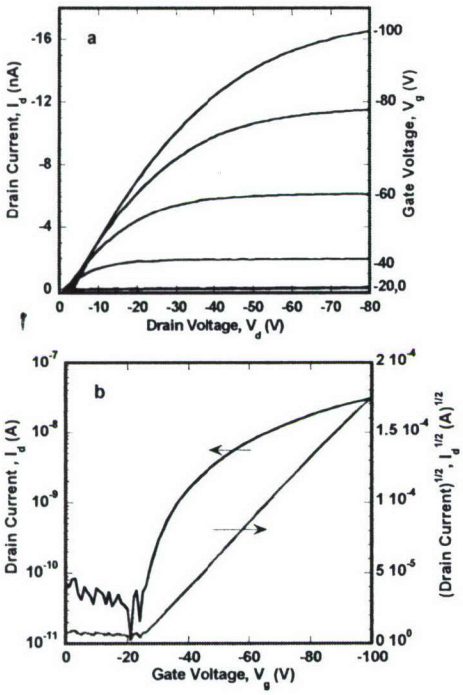

Fig. 34. The output characteristics (a) and transfer characteristics (b) of a HPT-HT FET.

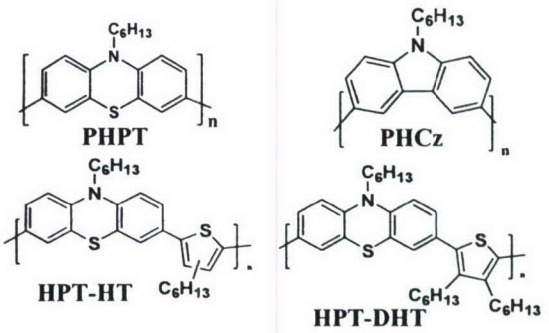

Fig. 33. Molecular structure of semiconducting polymers tested in *p*-channel FETs.

Transfer characteristics of a PHPT FET and a PHCz FET showed typical *p*-channel FET operating in the accumulation mode. The saturation region field-effect mobility of holes (μ_h) in PHCz was 1.5×10^{-5} cm^2/Vs and 7.5×10^{-6} cm^2/Vs in PHPT. A factor of 2 higher hole mobility in PHCz than in PHPT can be attributed to the relative coplanar structure of PHCz as compared to PHPT which possess a non-planar ring (dihedral angle ~ 158.5°).

Figure 34 shows the output and the transfer characteristics of a HPT-HT FET. The saturation region hole mobility for HPT-HT is 1×10^{-4} cm^2/Vs with I_{on}/I_{off} ratio of 10^3. More than an order of magnitude higher mobility of holes in HPT-HT copolymer as compared to the homopolymer suggests that the introduction of alkyl-thiophene moiety into the polymer backbone improves the ordering of the polymer chains. The devices made from HPT-DHT, where there are two alkyl side chains attached to the thiophene moiety, showed poor I-V characteristics with a field-effect mobility of holes of 1×10^{-7} cm^2/Vs. This reduction of hole mobility in HPT-DHT by three orders of magnitude as compared to HPT-HT is a result of increased steric hindrance to ordered stacking of polymer chains due to the two alkyl side chains.

These results show that conjugated polymers based on phenothiazine and carbazole are promising materials for solution-processed *p*-channel field-effect transistor applications. Although hole mobilities in the homopolymers are very low (~ 10^{-5} cm^2/Vs) we have shown that with proper structural modification through copolymerization higher charge carrier mobilities can be achieved. To further substantially increase the carrier mobilities, 2,7-linked polycarbazoles and 2,8-linked polyphenothiazines offer more linear chains with good prospects for better efficient π-stacking.

2.6 Synthesis and Theoretical Study of New High Electron Affinity Polymers.

One of the objectives of our synthetic efforts was to obtain new polymer semiconductors with high electron affinity (EA) to achieve Ohmic contacts from electrodes for facile electron injection in n-channel polymer field-effect transistors. We have successfully synthesized and characterized a new class of n-type conjugated polymers with very high electron affinity based on pyrazinoquinoxaline (Figure 35). The new poly(pyrazinoquinoxaline)s were fully characterized by NMR, FT-IR and UV-vis spectra. These polymers are soluble in formic acid, trifluoroacetic acid and other protonic acids.

All the poly(pyrazinoquinoxaline)s showed highly reversible reduction peaks and irreversible oxidation peaks. Figure 36 shows representative reduction cyclic voltammograms of PZQP and PZQT thin films. The formal reduction potentials of these polymers were in the range of -1.13 to -0.80 V vs SCE. The electron affinity of the poly(pyrazinoquinoxaline)s was 3.6-3.9 eV. These electron affinity values of the poly(pyrazinoquinoxaline)s are much higher than all currently known n-type conjugated polymers except ladder BBL and semiladder BBB. The ionization potential was estimated to be 5.8-6.1 eV. These results demonstrated that the pyrazinoquinoxaline moiety is an excellent building block for realizing high electron affinity organic semiconductors. A communication has been accepted for publication [11].

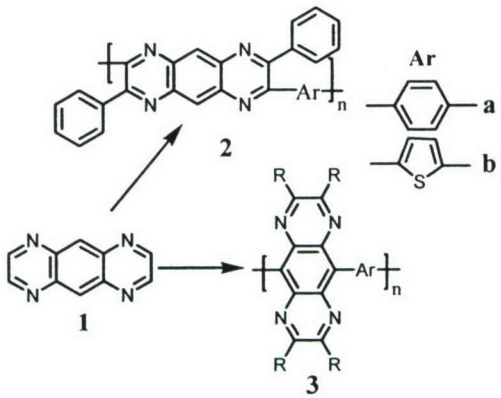

Fig. 35. Molecular structures of two classes of conjugated polymers derived from pyrazino quinoxaline (**1**) building block.

The electronic structures (HOMO/LUMO energy levels, band gaps, and bandwidths) of PZQP, PZQT, and related poly(pyrazino(2,3-g)quinoxaline-5, 10-diyl)s in which the polypyrazinoquinoxaline is linked through the 5,10-positions (Figure 35) were calculated by the density functional theory for comparison with the experimental results.

The calculated HOMO levels and band gaps were in excellent agreement with measured values while the calculated LUMO levels underestimated the experimental data for PZQP and PZQT by 17 %. The calculated electronic structures of thiophene-linked poly(pyrazino(2,3-g)quinoxaline-5, 10-diyl) (PZQT(5,10)) had a larger LUMO level (3.69 eV), a smaller HOMO level (4.33 eV) and thus a much smaller band gap (0.64 eV) compared with those of PZQT. The calculated effective masses for holes and electrons in the case of PZQT(5,10) ($0.054m_e$ and $0.058m_e$, respectively) are even smaller than in polythiophene ($0.133m_e$, $0.138m_e$). This suggests that some of the polypyrazinoquinoxalines are very promising materials for achieving high carrier mobilities. These results also suggest that poly(pyrazino(2,3-g)quinoxaline-5, 10-diyl)s are excellent candidates for future synthesis and experimental investigation.

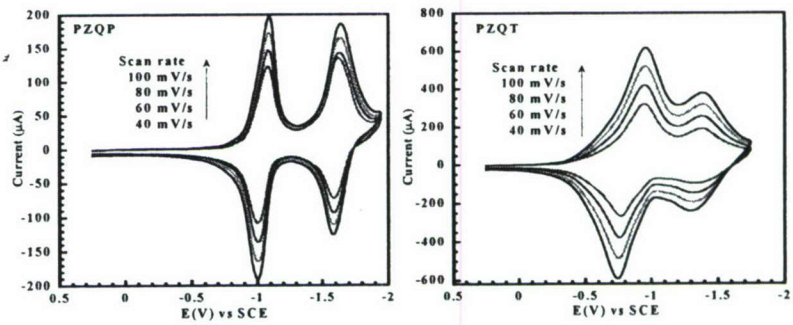

Fig. 36. Reduction cyclic voltammograms of PZQP and PZQT thin films in $TBAPF_6$/acetonitrile.

3. Publications Acknowledging AFOSR Grant (F49620-03-1-0162)

1. Babel, A.; Jenekhe, S. A. "Charge Carrier Mobility in Blends of Poly(9,9-dioctylfluorene) and Poly(3-hexylthiophene)," *Macromolecules* **2003**, *36*, 7759-7764.

2. Babel, A.; Jenekhe, S. A. "High Electron Mobility in Ladder Polymer Field Effect Transistors," *J. Am. Chem. Soc.* **2003**, *125*, 13656-13657.

3. Tonzola, C. J.; Alam, M. M.; Kaminsky, W.; Jenekhe, S. A. "New n-Type Organic Semiconductors: Synthesis, Single Crystal Structures, Cyclic Voltammetry, Photophysics, Electron Transport, and Electroluminescence of a Series of Diphenylanthrazolines," *J. Am. Chem. Soc.* **2003**, *125*, 13548-13558.

4. Zhu, Y.; Alam, M. M.; Jenekhe, S. A. "Regioregular Head-to-Tail Poly(4-alkylquinoline)s: Synthesis, Characterization, Self-Organization, Photophysics and Electroluminescence of New n-Type Conjugated Polymers," *Macromolecules* **2003**, *36*, 8958-8968.

5. Chen, W. C.; Liu, C. L.; Yen, C. T.; Tsai, F. C.; Tonzola, C. J.; Olson, N.; Jenekhe, S. A. "Theoretical and Experimental Characterization of Small Band Gap Poly(3,4-ethylenedioxythiophene methine)s," *Macromolecules* **2004**, *37*, 5959-5964.

6. Kwon, T. W.; Alam, M. M.; Jenekhe, S. A. "*n*-Type Conjugated Dendrimers: Convergent Synthesis, Photophysics, Electroluminescence and Use as Electron Transport Materials for Light Emitting Diodes," *Chem. Mater.* **2004**, *16*, 4657-4666.

7. Alam, M. M.; Jenekhe, S. A. "Efficient Solar Cells from Layered Nanostructures of Donor and Acceptor Conjugated Polymers," *Chem. Mater.* **2004**, *16*, 4647-4656.

8. Kulkarni, A. P.; Tonzola, C. J.; Babel, A.; Jenekhe, S. A. "Electron Transport Materials for Organic Light Emitting Diodes," *Chem. Mater.* **2004**, *16*, 4556-4573.

9. Babel, A.; Wind, J. D.; Jenekhe, S. A. "Ambipolar Charge Transport in Air-Stable Polymer Blend thin Film Transistors," *Adv. Funct. Mater.* **2004**, *14*, 891-898.

10. Li, D.; Babel, A.; Jenekhe, S. A.; Xia, Y. N. "Nanofibers of Conjugated Polymers Prepared by Electrospinning with a Two-Capillary Spinneret," *Adv. Mater.* **2004**, *16*, 2062-2066.

11. Zhu, Y.; Yen, C. T.; Jenekhe, S. A.; Chen, W. C. "Poly(pyrazinoquinoxaline)s: New n-Type Conjugated Polymers with Highly Reversible Reduction and High Electron Affinity," *Macromol. Rapid Commun.* **2004**, *25*, 1829-1834.

12. Babel, A.; Jenekhe, S. A. "Morphology and Field-Effect Mobility of Charge Carriers in Binary Blends of Poly(3-hexylthiophene) with Poly-[2-methoxy-5-(2-ethylhexoxy)-1,4-phenylene vinylene] and Polystyrene," *Macromolecules* **2004**, *37*, 9835-9840.

13. Babel, A.; Jenekhe, S. A. "Alkyl Chain Length Dependence of the Field-Effect Carrier Mobility in Regioregular Poly(3-Alkylthiophene)s," *Synth. Met.* **2005**, *148*, 169-173.

14. Babel, A.; Li, D.; Xia, Y.; Jenekhe, S. A. "Electrospun Nanofibers of Blends of Conjugated Polymers: Morphology, Optical Properties, and Field-Effect Transistors," *Macromolecules* **2005**, *38*, 4705-4711.

15. Zhu, Y.; Babel, A.; Jenekhe, S. A. "Phenoxazine-Based Conjugated Polymers: A New Class of Organic Semiconductors for Field-Effect Transistors," *Macromolecules* **2005**, *38*, 7983-7991.

16. Chang, C. C.; Pai, C. L.; Chen, W. C.; Jenekhe, S. A. "Spin Coating of Conjugated Polymers for Electronic and Optoelectronic Applications," *Thin Solid Films* **2005**, *479*, 254-260.

17. Tsai, F. C.; Chang, C. C.; Liu, C. L.; Chen, W. C.; Jenekhe, S. A. "New Thiophene-Linked Conjugated Poly(azomethine)s: Theoretical Electronic Structure, Synthesis, and Properties," *Macromolecules* **2005**, *38*, 1958-1966.

18. Kulkarni, A. P.; Zhu, Y.; Jenekhe, S. A. "Quinoxaline-Containing Polyfluorenes: Synthesis, Photophysics, and Stable Blue Electroluminescence," *Macromolecules* **2005**, *38*, 1553-1563.

19. Ponce Ortiz, R.; Malavé Osuna, R.; Ruiz Delgado, M. C.; Casado, J.; Jenekhe, S. A.; Hernandez, V.; Lopéz Navarrete, J. T. "Spectroscopic and DFT Studies of Donor–Acceptor Molecules Containing Phenylquinoline and Phenothiazine Moieties in Various Redox States," *Int. J. Quantum Chem.* **2005**, *104*, 635-644.

20. Kulkarni, A. P.; Wu, P. T.; Kwon, T. W; Jenekhe, S. A. "Phenothiazine-Phenylquinoline Donor-Acceptor Molecules: Effects of Structural Isomerism on Charge Transfer Photophysics and Electroluminescence," *J. Phys. Chem. B* **2005,** *109,* 19584-19594.

21. Zhu, Y.; Kulkarni, A. P.; Jenekhe, S. A. "Phenoxazine–Based Emissive Donor–Acceptor Materials for Efficient Organic Light Emitting Diodes," *Chem. Mater.* **2005**, *17*, 5225-5227.

22. Tonzola, C. J.; Hancock, J. M.; Babel, A.; Jenekhe, S. A. "Quinoidal Oligoquinoline: A Novel Quinodimethane Exhibiting High Electroluminescence Efficiency and p-Channel Field Effect Charge Transport," *Chem. Comm.* ***2005****, 41,* 5214-5216.

23. Tonzola, C. J.; Alam, M. M.; Jenekhe, S. A. "A New Synthetic Route to Soluble Polyquinolines with Tunable Photophysical, Redox, and Electroluminescent Properties," *Macromolecules* **2005,** *38,* 9539-9547.

24. Champion, R. D.; Cheng, K. F.; Pai, C. L.; Chen, W. C.; Jenekhe, S. A. "Electronic Properties and Field-Effect Transistors of Thiophene–Based Donor–Acceptor Conjugated Copolymers," *Macromol. Rapid Commun.* **2005**, *26*, 1835-1840.

25. Pai, C.-L.; Liu, C.-L.; Chen, W.-C.; Jenekhe, S. A. "Electronic Structure and Properties of Alternating Donor-Acceptor Conjugated Copolymers: 3, 4-Ethylenedioxythiophene (EDOT) Copolymers and Model Compounds," *Polymer* **2006**, *47*, 699-708.

26. Kulkarni, A. P.; Kong, X.; Jenekhe, S. A. "High-Performance Organic Light-Emitting Diodes Based on Intramolecular Charge-Transfer Emission from Donor-Acceptor Molecules: Significance of Electron-Donor Strength and Molecular Geometry," *Adv. Funct. Mater.* **2006**, *16*, 1057-1066.

27. Zhu, Y.; Champion, R. D.; Jenekhe, S. A. "Conjugated Donor-Acceptor Copolymer Semiconductors with Large Intramolecular Charge Transfer: Synthesis, Optical Properties, Electrochemistry, and Field Effect Carrier Mobility of Thienopyrazine Based Copolymers," *Macromolecules* **2006**, *39*, 8712-8719.

28. Kulkarni, A. P.; Kong, X.; Jenekhe, S. A. "Polyfluorene Terpolymers Containing Phenothiazine and Fluorenone: Effects of Donor and Acceptor Moieties on Intrachain Energy and Charge Transfer Processes in the Photoluminescence and Electroluminescence of Multichromophore Copolymers," *Macromolecules* **2006**, *39*, 8699-8711.

29. Alam, M. M.; Jenekhe, S. A. "Binary blends of polymer semiconductors: Nanocrystalline Morphology Retards Energy Transfer and Facilitates Efficient White Electroluminescence," *Macromol. Rapid Commun.* **2006**, *27*, 2053-2059.

30. Zhu, Y.; Gibbons, K. M.; Kulkarni, A. P.; Jenekhe, S. A. "Polyfluorenes Containing Dibenzo[*a,c*]phenazine Segments: Synthesis and Efficient Blue Electroluminescence from Intramolecular Charge Transfer States," *Macromolecules* **2007**, *40*, 804-813.

31. Jenekhe, S. A.; Alam, M. M.; Zhu, Y.; Jiang, S.; Shevade, A. V. "Single-Molecule Nanomaterials from π-Stacked Side-Chain Conjugated Polymers." *Adv. Mater.* **2007**, *19*, 536-542.

32. Hancock, J. M.; Gifford, A. P.; Tonzola, C. J.; Jenekhe, S. A. "High-Efficiency Electroluminescence from New Blue-Emitting Oligoquinolines Bearing Pyrenyl or Triphenyl Endgroups,' *J. Phys. Chem. C* **2007**, *111*, 6875-6882.

33. Tonzola, C. J.; Kulkarni, A.P.; Gifford, A. P.; Kaminsky, W.; Jenekhe, S. A. "Blue-light-Emitting Oligoquinolines: Synthesis, Properties, and High-Efficiency Blue-Light-Emitting Diodes," *Adv. Funct. Mater.* **2007**, *17*, 863-874.

34. Briseno, A. L.; Mansfield, S. C. B.; Reese, C.; Hancock, J. M.; Xiong, Y.; Jenekhe, S. A.; Bao, Z.; Xia, Y. "Perylenediimide Nanowires and Their Use in Fabricating Field-Effect Transistors and Complementary Inverters," *Nano Lett.* **2007**, *7*, 2847-2853.

35. Babel, A.; Zhu, Y.; Cheng, K. F.; Chen, W. C.; Jenekhe, S. A. "High Electron Mobility and Ambipolar Charge Transport in Binary Blends of Donor and Acceptor Conjugated Polymers," *Adv. Funct. Mater.* **2007**, *17*, 2542-2549.

36. Ahmed, E.; Briseno, A. L.; Xia, Y.; Jenekhe, S. A. "High Mobility Single-Crystal Field-Effect Transistors from Bisindoloquinoline Semiconductors," *J. Am. Chem. Soc.* **2007**, submitted (9-26-07).

4. Scientific Personnel Supported and Honors/Awards/Degrees

a. Senior Personnel

Samson A. Jenekhe

b. Postdoctoral Research Associates:

John D. Wind

c. Graduate Students

Amit Babel (PhD, 12/2005; now with Intel Corp.), Yan Zhu (PhD, 2006; now with Hewlett Packard Co.), Christopher Tonzola (PhD, 2005; now with Hercules Inc.), Jessica Hancock, and Pei-Tzu Wu

d. Undergraduate Students:

Jessica Lembong

e. Honors/Awards/Degrees

Senior Personnel

Samson A. Jenekhe: Elected Fellow, American Association for the Advancement of Science (AAAS), 2003; Elected Fellow, American Physical Society (APS), 2003.

5. Report of Inventions

None.